

2×2 Phased Array Consisting of Square Loop Antennas For High Gain Wide Angle Scanning with Low Grating Lobes

Arpan Pal, *Member, IEEE*, Amit Mehta, *Senior Member, IEEE*, Dariush Mirshekar-Syakhali, *Fellow, IEEE*, and Hisamatsu Nakano, *Life Fellow, IEEE*

Abstract— A 2×2 array antenna comprised of conventional Hybrid High Impedance Surface (HHIS) based reconfigurable Square Loop Antennas (SLA) as elements is presented. The SLA element has four conducting arms and each arm is fed at the middle by vertical probes, which is connected to a 50 Ω port at the bottom of antenna ground plane. Thus, the SLA element has four feeding ports and it is capable of generating five distinct radiation patterns by using a combination of its feeding ports. Depending upon which of its four ports are excited it can provide four high gain off-boresight tilted beams (8.9 dBi at $\theta_{max}=36^\circ$) in four different quadrants of the space (Tilted Beam Mode). When all the four ports are simultaneously excited with phases of 0° , 0° , 180° and 180° , it provides an axial beam (6.5 dBi) at boresight (Axial Beam Mode). By combining these two modes the 2×2 array of SLAs can provide a scanning range of -60° to $+60^\circ$ in the elevation plane with high gain beams (14 dBi-11.2 dBi).

Index Terms— Array antennas, pattern reconfigurable antennas, grating lobes, beam scanning.

I. INTRODUCTION

In phased array antennas [1], multiple antenna elements are excited coherently. Using variable phase and amplitude distribution over the elements, the radiation pattern of the antenna can be shaped and steered. Over the last two decades phased array antennas are widely used in different military systems such as warships, aircrafts, armored vehicles and guided weapons [2]. Due to recent advances in civil wireless communication technologies, the use of phased array antennas is on the rise. They have been employed in various applications including range extension for base-stations and interference avoidance between communication cells. They are also used in 60 GHz radios [3], satellite TVs [4], synthetic aperture systems, and radio frequency identification (RFID)

[5]. According to phased array theory [6]-[10], the pattern of an array system is the product of the Array Factor (AF) and the element pattern of the array. Consequently, the gain and scanning range of a phased array antenna are a function of the radiation pattern of its single antenna element. Array system could enhance its pattern adaptive ability if it deploys antenna elements capable of providing reconfigurable radiation patterns. Various designs of single element pattern reconfigurable antennas have been investigated for producing multiple radiation patterns. In [11]-[15], different combination of RF switches are utilized along the turns of spiral antennas for achieving pattern reconfigurability. Planar Yagi-Uda antennas [16]-[17] consisting of single driven patch and multiple parasitic patches are also investigated for reconfigurable pattern applications. Additionally, printed Square Loop Antennas (SLA) [18]-[20] have been reported for beam steering applications. These SLAs utilize multiple feed points on the square loop for producing multiple radiation patterns which can be steered in space by using RF switches.

Thus, a phased array antenna containing such pattern reconfigurable antennas as elements can offer an additional (third) degree of freedom in the form of reconfigurable element pattern, besides amplitude and phase of the excitation signals. This additional degree of freedom enables the array antenna system to achieve a number of advantages. These include wider scanning range, faster beam scanning, high gain in the off boresight directions, choice of different types of modulations in RF domain for secure communications and lower grating or side lobes, etc. In [21]-[22], investigations on reduction of side lobe level of array with reconfigurable elements have been reported. In [23], beam steering of an array of switch-based spiral loop has been demonstrated for directional modulation. In [24]-[25], pattern reconfigurable microstrip Yagi antennas are used to extend the phased array scan range. A new class of antenna array of multifunctional reconfigurable antennas is presented in [26], which utilizes a parasitic layer to steer the beam. For wide angle scanning phased array systems are developed in [27]-[28] which utilize PIN and Varactor diodes for achieving pattern reconfigurability for an element.

In this paper, we focus on achieving high gain at off boresight directions and mitigating the grating lobes at wide

A. Pal and A. Mehta are with College of Engineering, Swansea University, Swansea, SA28PP, U.K. (email: a.pal@swansea.ac.uk, a.mehta@swansea.ac.uk).

D. Mirshekar-Syakhali is with the Department of Computing Science and Electronic Engineering, Essex University, Colchester, Essex CO4 3SQ, U.K. (e-mail: dariush@essex.ac.uk).

H. Nakano is with the Science and Engineering Department, Hosei University, Koganei, Tokyo 184-8584, Japan (e-mail: hysmat@hosei.ac.jp).

scan angles. The performance of a 2×2 phased array system consisting of pattern reconfigurable Square Loop Antennas (SLAs) is investigated. Each of these SLAs has five distinct element patterns: one axial beam and four tilted beams. The SLA unit element can provide these titled or axial beams independent of other unit element radiation patterns. This ability makes the SLA an excellent candidate for a sub-array to be a part of large phased array, for effectively compensating beam deviating in conformal array platforms. In this research, the antenna performances are simulated using CST Microwave studio, which is based on Finite Integration Technique in Time Domain (FIT-TD) [29]. The antenna prototype is fabricated using a standard photolithography technique and characterized using an Agilent Vector Network Analyzer (VNA). The radiation patterns are measured using Satimo's StarLab [30].

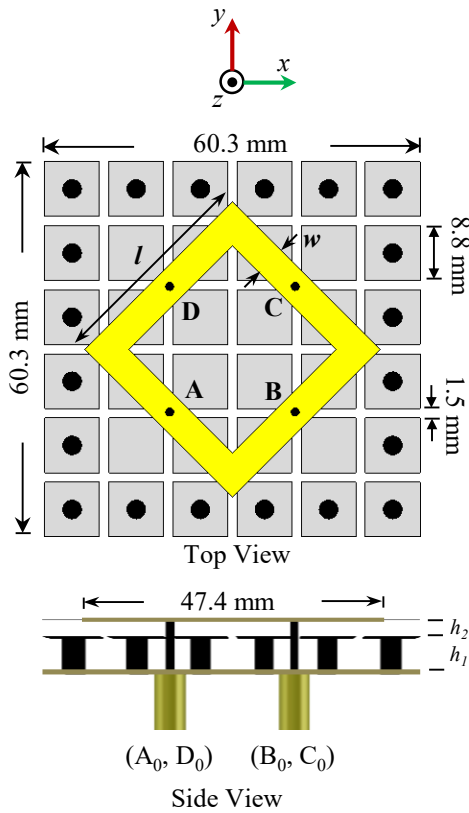


Fig. 1. Top and side views of the SLA element.

II. PATTERN RECONFIGURABLE SQUARE LOOP ANTENNA

Fig. 1 shows the top and side views of an array element (pattern reconfigurable SLA). The SLA has four conducting arms, each having length $l=33.5$ mm and track width $w=5$ mm. The loop is printed on a Rogers 4350B substrate ($\epsilon_r=3.48$, $\tan\delta=0.009$) which has a height of $h_2=1.52$ mm and this substrate layer is placed over a Hybrid High Impedance Surface (HHIS) [31]. The HHIS structure enables realization of low antenna profile. It is composed of a 6×6 array of square metal plates, where each square has a side length of 8.8 mm with a gap of 1.5 mm between neighboring metal plates. The squares plates on the outer periphery of the HHIS structure are shorted to the ground by metal vias, each having

a diameter of 3 mm. This arrangement reduces mutual coupling between array elements. In addition, it decreases the surface wave propagation in the substrate, which in turn reduces the side lobes [31]. The HHIS layer is etched on the top of Rogers 5880 substrate ($\epsilon_r=2.2$, $\tan\delta=0.009$) having a height of $h_1=3.18$ mm. Therefore, the SLA occupies an area of 60.3 mm×60.3 mm and has a total height of 4.7 mm (h_1+h_2). The whole antenna structure is backed by a conducting ground plane. The loop is fed at the center (A, B, C and D) of each arm using four vertical probes of 1.3 mm diameters, which are connected to the four feeding ports (standard 50 Ω SMA connectors) - (A_0 , B_0 , C_0 and D_0) at the bottom of the ground plane.

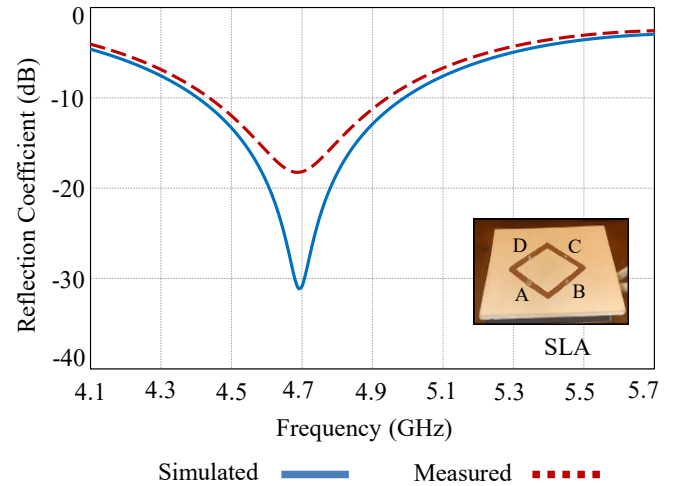


Fig. 2. Simulated and measured reflection coefficients of the element SLA. (inset) Fabricated prototype.

Fig. 2 shows the simulated and measured reflection coefficients of the SLA. The measured and simulated results for 50Ω feed are in good agreement. The reflection coefficients satisfy a criterion of $|S_{11}| < -10$ dB within a frequency range of 4.4 GHz to 5 GHz. Thus, the SLA has an impedance bandwidth of 600 MHz ($\approx 13\%$). Both simulated and measured reflection coefficients become minimum at 4.7 GHz, which is denoted as the test frequency throughout this paper.

Fig. 3 shows simulated and experimental 2D cuts of the radiation pattern of the SLA at 4.7 GHz. When one of the feeding ports (either A_0 , B_0 , C_0 or D_0) of SLA is excited and the remaining ports are open-circuited, the antenna generates a tilted beam of $\theta_{max}=36^\circ$ directed toward the opposite space quadrant of the excited port. Thus, with feeding port A_0 excited and others open-circuited a tilted beam with $\phi_{max}=45^\circ$ occurs (shown in Fig. 3a). Accordingly, when remaining three ports B_0 , C_0 and D_0 are excited individually the antenna generates a tilted beam of $\theta_{max}=36^\circ$ pointed in the direction of $\phi_{max}=135^\circ$, $\phi_{max}=225^\circ$ and $\phi_{max}=315^\circ$, respectively (shown in Fig. 3. c, d and f). Therefore, depending upon which of its feeding port is excited the SLA provides four titled beams in the four spatial quadrants. Since the square loop antenna is symmetrical with respect to the antenna center point, the tilted

beams are identical to each other. Each tilted beam provides a gain of 8.9 dBi in the direction of the maximum radiation field. The efficiency (including reflection) of the element SLA is found to be better than 97% over the impedance bandwidth. The main lobe of the tilted beam is linearly polarized in the θ -direction and the amplitude of the cross-polar components is very small (i.e.: $E_{\phi} \leq -20\text{dB}$ and thus not visible) in the direction of the main beam, which has a HPBW of approximately 60° .

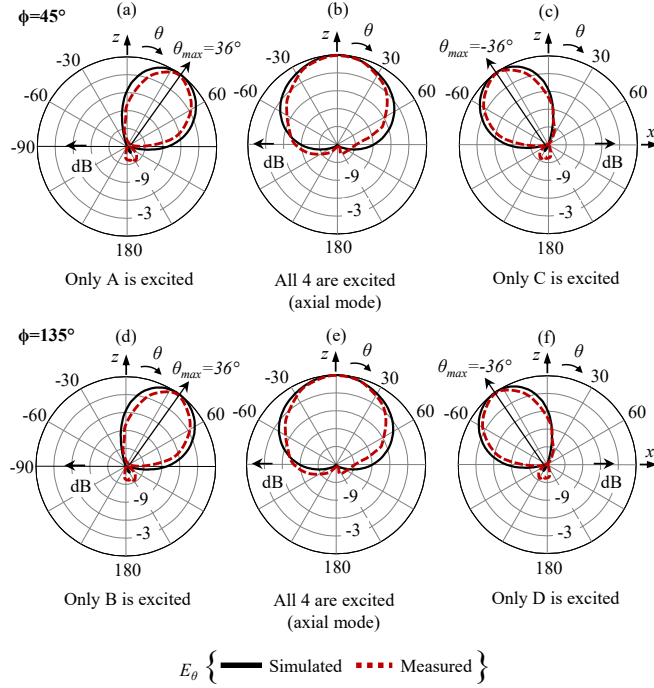


Fig. 3. Normalized radiation pattern of SLA at 4.7 GHz at $\phi=45^\circ$ and $\phi=135^\circ$ planes.

The fifth radiation beam of the SLA is an axial beam (single E_θ polarized), where all four ports A_0 , B_0 , C_0 and D_0 are excited simultaneously with equal amplitude and phases of 0° , 0° , 180° and 180° , respectively [32]-[33]. This phase relationship for extracting the axial beam from the SLA is denoted as ϕ_{axial} . The axial beam produced is shown in Figs. 3(b) and 3(e), where the gain is 6.5 dBi and the main lobe has a HPBW of 100° in the $\phi=45^\circ$ and $\phi=135^\circ$ planes.

From Fig. 3, we can ascertain that due to the switching feed geometry the SLA would offer truly single polarization (E_θ) for beam steering in the elevation and azimuth planes. This property is very important when the array antenna system tracks a source moving around the azimuth plane with single vertical transmit polarization. In the following section, the performances of 2×2 array SLAs are presented.

III. ARRAY CONFIGURATION AND REFLECTION COEFFICIENT

The array of SLAs utilizes the aforementioned five different element patterns. As shown in Fig. 3, in the $\phi=45^\circ$ plane the array of SLAs can use three distinct element patterns. A tilted beam of $\theta_{\text{max}}=36^\circ$ due to port A excitation, an axial beam, and a tilted beam of $\theta_{\text{max}}=-36^\circ$ due to port C to scan the entire elevation plane. Similarly, to scan in the $\phi=135^\circ$ plane an axial

beam and two tilted beams due to port B and D excitations are exploited. The radiation pattern bandwidth for the five patterns of the SLA also holds good over the impedance bandwidth.

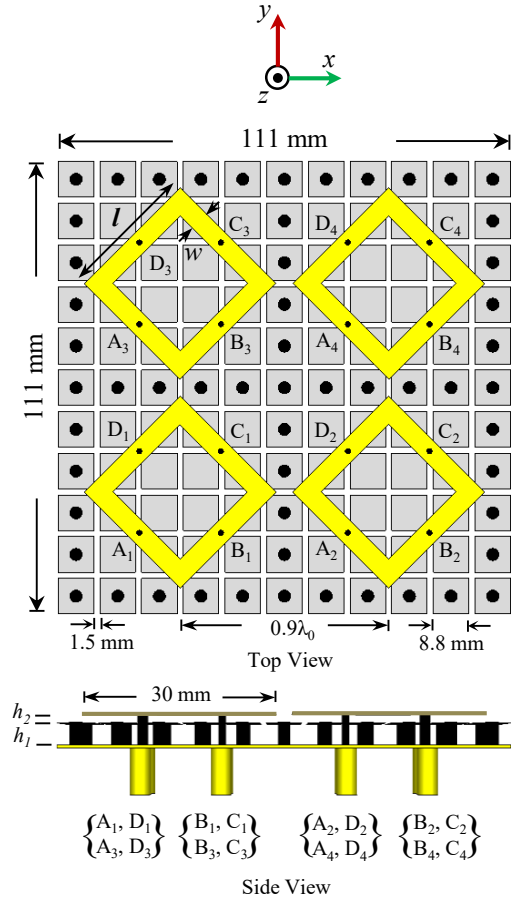


Fig. 4. 2×2 array of SLAs

Fig. 4 shows a 2×2 array of SLAs. Each SLA has the identical dimensions as shown in Fig. 1. The HHIS structure is composed of 11×11 square metal plates with the similar specification as stated in Fig. 1. Each small metal plate on the outer periphery of HHIS is short-circuited to the ground by a conducting (copper) via of 3 mm diameter. These vias enable the array to reduce surface wave propagation in the structure [31]. In addition, there are two rows of vias that run through the middle of the HHIS structure, which separate each square loop from the adjacent loops and reduce the mutual coupling between the square loops. The overall planar size of the array is $111 \text{ mm} \times 111 \text{ mm}$ with a height of 4.7 mm (h_1+h_2). The lateral (diagonal) dimension of the square loop is $0.75\lambda_0$ (47.4 mm), (where the free space wavelength at the test frequency 4.7 GHz is $\lambda_0 \approx 64 \text{ mm}$). The distance between the centers of two adjacent elements is selected as $0.9\lambda_0$ at the test frequency. With four feeding ports for each element the array system has 16 ports, which are connected to the SMA ports. These ports are labelled as (A_1, B_1, C_1, D_1) , (A_2, B_2, C_2, D_2) , (A_3, B_3, C_3, D_3) and (A_4, B_4, C_4, D_4) .

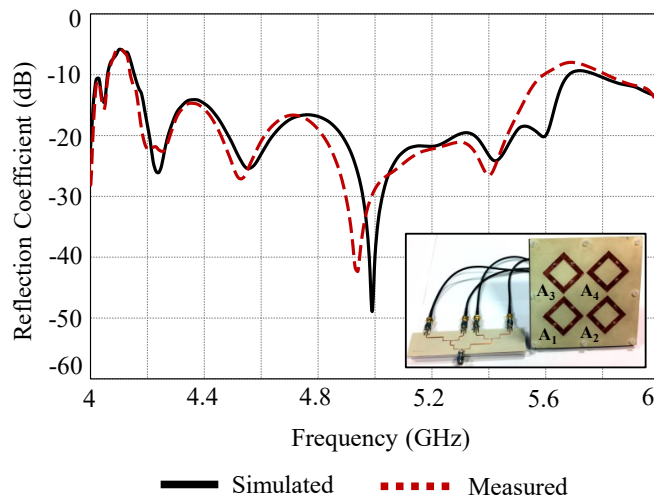


Fig. 5. Simulated and measured reflection coefficients of a 2×2 array of SLAs integrated with the feeding network (port A1-A4 excited). (inset) Prototype.

Fig. 5 shows the simulated and measured reflection coefficients ($|S_{11}|$) of the array excited at ports A_s ($s=1, 2, 3$ and 4). The feeding network was designed to excite the four A_s ports with the signal of equal amplitude and a specific phase relationship for generating a beam in the $\theta_{\max}=60^\circ$ direction. Fig. 5 shows that the array with its feeding network provides efficient radiation with $|S_{11}| < -10$ dB across an impedance bandwidth of 4.2 to 5.6 GHz. The reflection coefficients of the other tilted beams (excited through ports B, C and D individually) and the axial mode beam (ports A, B, C and D are excited simultaneously) were found to be $|S_{11}| < -10$ dB over the impedance bandwidth. For succinctness, they are not presented.

The experimental feeding networks for providing phase shifts were designed using delay lines (instead of variable electronic phase shifters), Fig. 5 (inset), which had total power dissipation of 0.9 dB at the test frequency. The phase shifting (delay) lines were etched on the top of Rogers's 4003C substrate ($\epsilon_r=3.38$, $\tan\delta=0.0027$ and thickness=0.508mm) backed by a ground plane. The radiation pattern bandwidth is discussed in Section IV.

IV. SCAN PERFORMANCE OF THE 2×2 ARRAY

To synthesize the radiation pattern for the 2×2 planar array, the elements of the array are arranged in the x - and y -directions. Two adjacent elements of the array are separated by $0.9 \lambda_0$ distance in the x - and y - directions, respectively. The elements are excited with signals of equal amplitude and phase shifts of $\Delta\theta_x$ and $\Delta\theta_y$ in the x - and y - directions, respectively. The phase relationship of the 16 excited ports at the test frequency is shown in Fig. 6.

The beam scanning performance of the array in the elevation and azimuth planes are examined. For test, an elevation plane cut is performed at $\phi=45^\circ$ and an azimuth plane cut is performed at $\theta=30^\circ$. The limit for the magnitude of the grating lobes is set to be -10 dB down from that of the

main lobe. This is an essential criterion to ensure that in the transmitting mode the array does not cause interference in unwanted directions. Similarly, in the receiving mode this ensures that the antenna system does not pick up jamming signals through unwanted grating lobe directions.

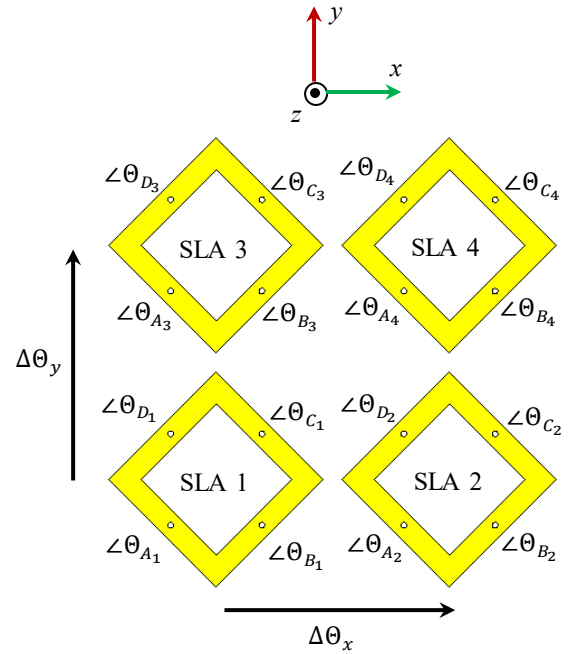
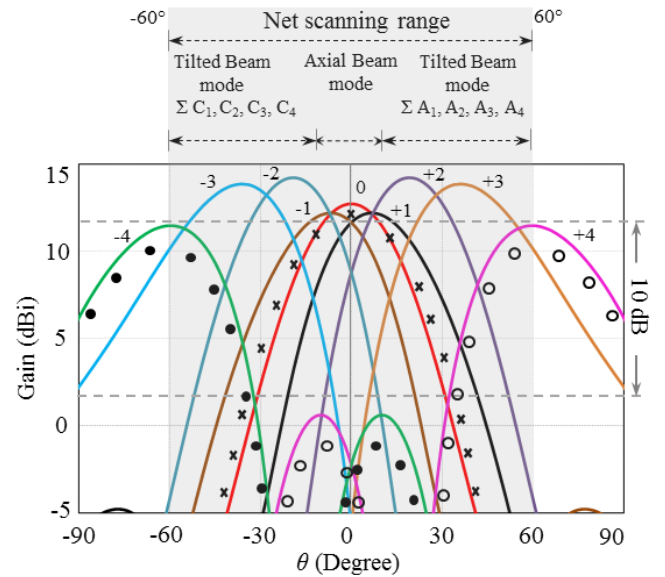


Fig. 6. Phase relationship of the 16 ports.



Simulated θ_{\max} :

Axial mode { -1 -10° 0 0° $+1$ 10° }

Tilted mode { -4 -60° -3 -35° -2 -19° $+2$ 19° $+3$ 35° $+4$ 60° }

Measured θ_{\max} :

Axial mode { $\times \times \times 0^\circ$ } Tilted mode { $\bullet \bullet \bullet -60^\circ$ $\circ \circ \circ 60^\circ$ }

Fig. 7. Beam scanning of the 2×2 array of SLAs at $\phi=45^\circ$.

A. Elevation plane (at $\phi=45^\circ$) scanning

The array has two scanning modes: axial beam mode and tilted beam mode. For the axial beam mode, all 16 ports need to be excited simultaneously, with the condition that the four ports of every individual SLA are in ' ϕ_{axial} ' phase relation. ' ϕ_{axial} ' was denoted in section II where the phase shift relationship is as follows: $\angle\theta_{A_{1,2,3,4}} = \angle\theta_{B_{1,2,3,4}} = 0^\circ$ and $\angle\theta_{C_{1,2,3,4}} = \angle\theta_{D_{1,2,3,4}} = 180^\circ$. Fig. 7 shows the beam scanning of the 2×2 array of SLAs in the $\phi=45^\circ$ elevation plane for both the tilted and the axial beam modes. In the axial beam mode the array provides a linear polarized beam with a gain of 12.7 dBi. The axial beam is steered in the elevation plane by introducing a phase shift between the SLAs. It was found that if a phase shift of $\Delta\theta_x = \Delta\theta_y = \pm 40^\circ$ are introduced between the SLAs, the axial beam is steered in a range of $\theta_{\text{max}} = \pm 10^\circ$ with a minimum gain of 11.6 dBi. Scanning beyond this axial steering range causes grating lobes to become dominant. Hence, by axial beam mode the array scans in the elevation plane from -10° to 10° . This is shown in the middle of Fig. 7.

For the tilted beam mode scanning, depending upon the quadrant, only four ports are excited at a time and the remaining ports are left open-circuited. For example, for beam scanning in the quadrant of $0^\circ < \phi < 90^\circ$, only the four A ports (A_1 - A_4) need to be excited. It was found that when the excitations of four A ports (A_1 - A_4) are combined together with the phase shifts of $\Delta\theta_x = \Delta\theta_y = -40^\circ$, the array provides the radiation beam in a direction of $\theta_{\text{max}} = 19^\circ$ with a gain of 14.2 dBi. This is shown on the right side of Fig 7. The grating lobe levels are below -10 dB from that of the main beam. When the phase shifts are set to be $\Delta\theta_x = \Delta\theta_y = -230^\circ$, the antenna exhibits a radiation beam in a direction of $\theta_{\text{max}} = 60^\circ$. This beam has a gain of 11.5 dBi with grating lobe level still below that of -10dB. The grating lobes started to become dominant if the beam was scanned beyond this upper limit. Hence, by exciting (A_1 - A_4) simultaneously the array scans the beam from $\theta_{\text{max}} = 19^\circ$ to $\theta_{\text{max}} = 60^\circ$ in the $\phi = 45^\circ$ plane.

Similarly with the same phase shifts, the other half of the elevation plane; i.e. $\phi = 225^\circ$, can be easily scanned by using four C ports (C_1 - C_4). This is shown in the left side of Fig. 7. It shows that by exciting four C ports simultaneously the antenna scans its beam from $\theta_{\text{max}} = -19^\circ$ to $\theta_{\text{max}} = -60^\circ$ (lower limit of tilted steering range). Fig. 7 also shows the measured radiation patterns undertaken for $\theta_{\text{max}} = \pm 60^\circ$. This validates the titled steering mode. Hence, combining the axial and tilted beam mode together a full scanning range of $\pm 60^\circ$ is achieved. It should be noted that a region between $-19^\circ < \theta_{\text{max}} < -10^\circ$ and a region between $+10^\circ < \theta_{\text{max}} < +19^\circ$ will be covered by the tilted beam mode. This has a gain of 14.2 dBi at $\theta_{\text{max}} = \pm 19^\circ$ and a gain of 11.6 dBi at $\theta_{\text{max}} = \pm 10^\circ$. For succinctness, the results in this paper are only shown for $\phi=45^\circ$ / $\phi=225^\circ$ elevation planes. Due to symmetry of the antenna structure with respect to the center point of the antenna, the identical results are observed for other planes. For ready reference the phase values for different feeding ports for elevation plane scanning in a $\phi=45^\circ$ plane are provided in Table I.

Table I. Excitation phase values for elevation plane scanning at $\phi=45^\circ$. (-: open-circuit / not excited)

	Tilted beam mode			Axial beam mode			Tilted beam mode		
θ_{max}	-60°	-35°	-19°	-10°	0°	10°	19°	35°	60°
$\angle\theta_{A_1}$	-	-	-	0°	0°	0°	0°	0°	0°
$\angle\theta_{B_1}$	-	-	-	0°	0°	0°	-	-	-
$\angle\theta_{C_1}$	0°	0°	0°	180°	180°	180°	-	-	-
$\angle\theta_{D_1}$	-	-	-	180°	180°	180°	-	-	-
$\angle\theta_{A_2}$	-	-	-	40°	0°	-40°	-40°	-125°	-230°
$\angle\theta_{B_2}$	-	-	-	40°	0°	-40°	-	-	-
$\angle\theta_{C_2}$	230°	125°	40°	220°	180°	140°	-	-	-
$\angle\theta_{D_2}$	-	-	-	220°	180°	140°	-	-	-
$\angle\theta_{A_3}$	-	-	-	40°	0°	-40°	-40°	-125°	-230°
$\angle\theta_{B_3}$	-	-	-	40°	0°	-40°	-	-	-
$\angle\theta_{C_3}$	230°	125°	40°	220°	180°	140°	-	-	-
$\angle\theta_{D_3}$	-	-	-	220°	180°	140°	-	-	-
$\angle\theta_{A_4}$	-	-	-	80°	0°	-80°	-80°	-250°	-460°
$\angle\theta_{B_4}$	-	-	-	80°	0°	-80°	-	-	-
$\angle\theta_{C_4}$	460°	250°	-80°	260°	180°	100°	-	-	-
$\angle\theta_{D_4}$	-	-	-	260°	180°	100°	-	-	-

B. Azimuth plane (at $\theta=30^\circ$) scanning

Fig. 8 shows the scan performance of the 2×2 array in the azimuth plane at $\theta=30^\circ$ at the test frequency. To cover the quadrant of $0^\circ < \phi < 90^\circ$ the four A ports (A_1 - A_4) are needed to be excited. When the ports (A_1 - A_4) are fed with the phase shift of $\Delta\theta_x = -160^\circ$ and $\Delta\theta_y = 0^\circ$ the maximum radiation is directed toward a direction of $\phi_{\text{max}}=15^\circ$. The main beam is steered to $\phi_{\text{max}}=75^\circ$ with the phase shifts of $\Delta\theta_x = 0^\circ$ and $\Delta\theta_y = -160^\circ$. Hence, by exciting four A ports the array scans a region of $15^\circ < \phi_{\text{max}} < 75^\circ$ with grating lobes of less than -10 dB. It is noticed that the gain of the array is maximum (14.2 dBi) at $\phi_{\text{max}}=45^\circ$ and reduces to 13.2 dBi at $\phi_{\text{max}}=15^\circ$ and $\phi_{\text{max}}=75^\circ$. Similarly, as shown in the Fig. 8 the array also covers a region of $105^\circ < \phi < 165^\circ$, $195^\circ < \phi < 255^\circ$ and $285^\circ < \phi < 345^\circ$ in the azimuth plane when the (B_1 - B_4), (C_1 - C_4) and (D_1 - D_4) ports are excited, respectively. For ready reference, the phase values and their inter-relationships for the feeding ports are tabulated in Table II. Thus, by switching amongst the ports with right phases the array scans nearly 360° of the azimuth plane at an off boresight direction of $\theta_{\text{max}}=30^\circ$, with gain varying between 14.2 dBi to 13.2 dBi. The remaining region in the azimuth plane is covered with a relatively low gain (13.2-12.9 dBi), as shown in the grey zone. If a high gain (~ 14 dBi) beam scanning in the grey region is required, then

an 8 beam element antenna is needed, as conceptualized in [35].

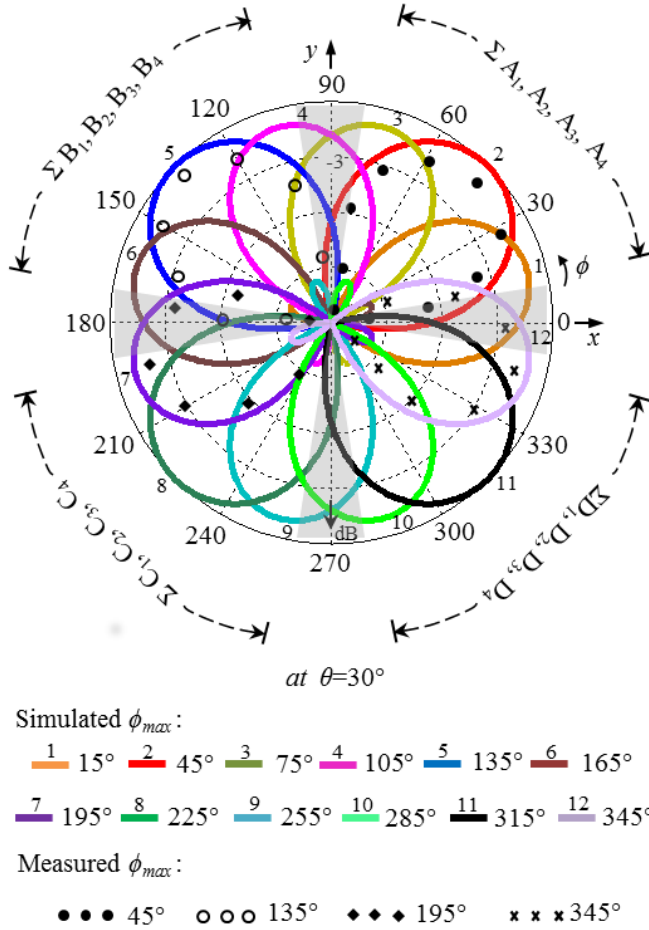


Fig. 8. Azimuth beam scanning of the 2x2 array of SLAs at $\theta=30^\circ$.

Fig 9 shows the efficiency (including reflection) and gain for the axial beam mode ($\theta_{max} = 0^\circ$). The array provides an axial beam with an efficiency of more than 70% within a range of 4.4 to 5.1 GHz. For this frequency range the gain varies from 11.5 to 10 dBi. Beyond 5.1 GHz the sidelobe magnitude increases. Fig. 10 shows the efficiency and gain in the $(\theta_{max}, \phi_{max}) = (60^\circ, 45^\circ)$ direction. The array provides a tilted beam with an efficiency of more than 70% within a range of 4.6 to 5.25 GHz. Within this range the gain varies from 11 to 11.5 dBi.

V. CONCLUSION

A study of the scanning performance of a 2x2 array consisting of HHIS-based reconfigurable Square Loop Antenna (SLA) elements is presented. The unit element SLA has four feeding ports and depending upon their combination (either one at a time or all four simultaneously), it has five distinct patterns. It provides 4 tilted beams (8.9 dBi at $\theta_{max}=36^\circ$) in four quadrants of space and an axial beam (6.5 dBi at $\theta_{max}=0^\circ$). The array of SLAs utilizes both of these tilted

and axial beam modes for beam scanning operation. By combining these two modes, the array is capable of scanning a range of -60° to $+60^\circ$ in the elevation plane. In this scanning range, a maximum gain of 14.2 dBi and a minimum gain of 11.5 dBi are observed. In addition, the array also performs a full azimuth scan in the off boresight direction of $\theta_{max}=30^\circ$, with gains varying between 14.2 dBi to 13.2 dBi. In both elevation and azimuth scans the magnitude of grating lobe stays below -10 dB. This advantage is significant when the array is deployed for off-boresight high-gain wide angle scanning with low grating lobes.

Table II. Phase values for azimuth plane scanning at $\theta_{max}=30^\circ$.

Scanning $0^\circ < \phi < 90^\circ$ using $A_{1,2,3,4}$ excitations $B_{1,2,3,4}$, $C_{s1,2,3,4}$ and $D_{1,2,3,4}$ ports = not excited / open-circuited			
ϕ_{max}	15°	45°	75°
$\angle \theta_{A_1}$	0°	0°	0°
$\angle \theta_{A_2}$	-160°	-100°	0°
$\angle \theta_{A_3}$	0°	-100°	-160°
$\angle \theta_{A_4}$	-160°	-200°	-160°
Scanning $90^\circ < \phi < 180^\circ$ using $B_{1,2,3,4}$ excitations $A_{1,2,3,4}$, $C_{s1,2,3,4}$ and $D_{1,2,3,4}$ ports = not excited / open-circuited			
ϕ_{max}	105°	135°	165°
$\angle \theta_{B_1}$	0°	0°	0°
$\angle \theta_{B_2}$	0°	100°	160°
$\angle \theta_{B_3}$	-160°	-100°	0°
$\angle \theta_{B_4}$	-160°	0°	160°
Scanning $180^\circ < \phi < 270^\circ$ using $C_{1,2,3,4}$ excitations $A_{1,2,3,4}$, $B_{1,2,3,4}$ and $D_{1,2,3,4}$ ports = not excited / open-circuited			
ϕ_{max}	195°	225°	255°
$\angle \theta_{C_1}$	0°	0°	0°
$\angle \theta_{C_2}$	160°	100°	0°
$\angle \theta_{C_3}$	0°	100°	160°
$\angle \theta_{C_4}$	160°	200°	160°
Scanning $270^\circ < \phi < 360^\circ$ using $D_{1,2,3,4}$ excitations $A_{1,2,3,4}$, $B_{s1,2,3,4}$ and $C_{1,2,3,4}$ ports = not excited / open-circuited			
ϕ_{max}	285°	315°	345°
$\angle \theta_{D_1}$	0°	0°	0°
$\angle \theta_{D_2}$	0°	-100°	-160°
$\angle \theta_{D_3}$	160°	100°	0°
$\angle \theta_{D_4}$	160°	0°	-160°

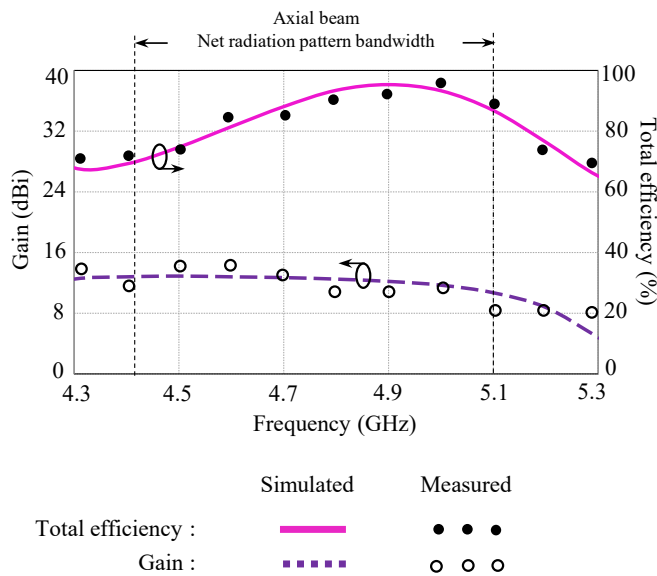


Fig. 9. Gain and total efficiency of the 2x2 array of SLAs (axial beam mode) at $(\theta_{max}, \phi_{max}) = (0^\circ, 45^\circ)$.

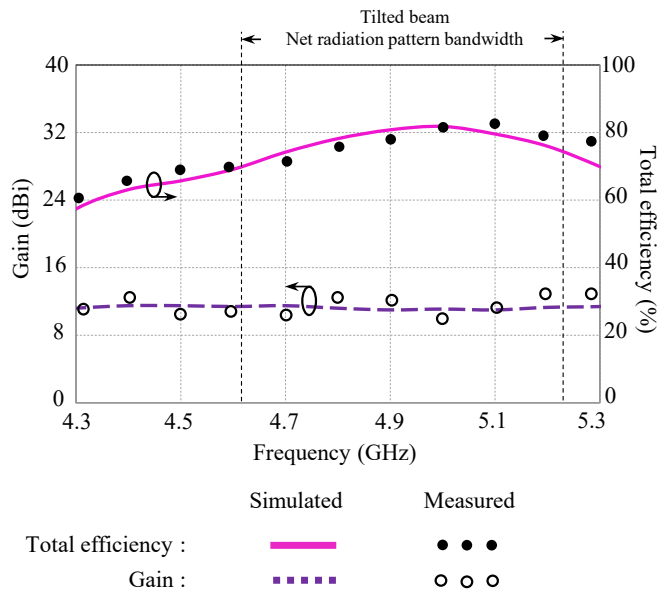


Fig. 10. Gain and efficiency of the 2x2 array SLAs (tilted beam mode) at $(\theta_{max}, \phi_{max}) = (60^\circ, 45^\circ)$.

REFERENCES

- [1] A. J. Fenn, D. H. Temme, W. P. Delaney and W. E. Courtney, "The development of phased-array radar technology," *Lincoln Lab. J.*, vol. 12, no. 2, pp. 321-340 2000
- [2] E. Rai, S. Nishimoto, T. Katada and H. Watanabe, "Historical overview of phased array antennas for defense application in Japan," *IEEE Int. Symp. on Phased Array Systems and Technology Digest*, vol., pp. 217-221, 15-18 Oct. 1996.
- [3] B. Zhang, Y. P. Zhang, D. Titz, F. Ferrero and C. Luxey, "A circularly-polarized array antenna using linearly-polarized sub grid arrays for highly-integrated 60-GHz radio," *IEEE Trans. Antennas and Propag.*, vol. 61, no.1, pp.436-439, Jan. 2013.
- [4] H. Mitsumoto, T. Murata, K. Takano, M. Fujita, S. Tanaka, S. Itoh, K. Shogen, N. Toyama and H. Miyazawa, "A mobile satellite news

- gathering system using a flat antenna," *IEEE Trans. Broadcasting*, vol. 42, no. 3, pp.272-277, Sep. 1996.
- [5] A. Buffi, A. A. Serra, P. Nepa, H. T. Chou and G. Manara, "A focused planar microstrip array for 2.4 GHz RFID readers," *IEEE Trans. Antennas and Propag.*, vol.58, no.5, pp.1536-1544, May. 2010.
- [6] R. J. Mailloux, J. F. McIlvenna and N. Kernweis, "Microstrip array technology," *IEEE Trans. Antennas and Propag.*, vol. 29, no.1, pp. 25-37, Jan. 1981.
- [7] Z. Zhang and L. Jin, "Radar Antenna Technology," Beijing, China: Publishing House of Electronics Industry, 2007.
- [8] S. Chattopadhyay, J. Y. Siddiqui and D. Guha, "Rectangular microstrip patch on a composite dielectric substrate for high-gain wide-beam radiation patterns," *IEEE Trans. Antennas and Propag.*, vol.57, no.10, pp.3325-3328, Oct. 2009.
- [9] G. Lin, "A wide-beam antenna element for phased-array," *Radar Sci. Technol.*, vol. 5, no. 2, pp. 157-160, Apr. 2007.
- [10] R. L. Haupt, "Antenna arrays: a computational approach", Wiley-IEEE Press, 2010.
- [11] G. H. Huff, J. Feng, S. Zhang and J. T. Bernhard, "A novel radiation pattern and frequency reconfigurable single turn square spiral microstrip antenna," *IEEE Microw. Wireless Compon. Lett.*, vol.13, no.2, pp.57-59, Feb. 2003.
- [12] A. Mehta and D. Mirshekar-Syahkal, "Spiral antenna with adaptive radiation pattern under electronic control," *IEEE Int. Symp. on Antennas and Propag. Soc. Digest*, vol. 1, pp. 843-846, Jun. 2004.
- [13] A. Mehta, D. Mirshekar-Syahkal and H. Nakano, "Beam adaptive single arm rectangular spiral antenna with switches," *IEE Proc.-Microwaves, Antennas and Propagation*, vol.153, no.1, pp.13-18, Feb. 2006.
- [14] C. W. Jung, M. J. Lee, G. P. Li and F. De Flaviis, "Reconfigurable scan-beam single-arm spiral antenna integrated with RF-MEMS switches," *IEEE Trans. Antennas and Propag.*, vol. 54, no. 2, pp. 455-463, Feb. 2006.
- [15] G. H. Huff and J. T. Bernhard, "Integration of packaged RF MEMS switches with radiation pattern reconfigurable square spiral microstrip antennas," *IEEE Trans. Antennas and Propag.*, vol. 54, no. 2, pp. 464-469, Feb. 2006.
- [16] X. S. Yang, B. Z. Wang, W. Wu and S. Xiao, "Yagi patch antenna with dual-band and pattern reconfigurable characteristics," *IEEE Antennas Wireless Propag. Lett.*, vol. 6, pp. 168-171, Apr. 2007.
- [17] S. K. Sharma, F. Fideles and A. Kalikonda, "Radiation pattern reconfigurable planar Yagi-Uda antenna," *IEEE Antennas and Propag. Soc. Int. Symp. (APSURSI) Digest*, pp.190-191, 7-13 July 2013.
- [18] A. Mehta and D. Mirshekar-Syahkal, "Pattern steerable square loop antenna," *Electron. Letts.*, vol.43, no.9, pp.491-493, Apr. 2007.
- [19] A. Pal, A. Mehta, D. Mirshekar-Syahkal and P. J. Massey, "Short-circuited feed terminations on beam steering square loop antennas," *Electron. Letts.*, vol.44, no.24, pp.1389-1390, Nov. 2008.
- [20] A. Pal, A. Mehta, D. Mirshekar-Syahkal, P. Deo, H. Nakano, "Dual-band low-profile capacitively coupled beam-steerable square-loop antenna," *IEEE Trans. Antennas and Propag.*, vol.62, no.3, pp.1204-1211, March 2014.
- [21] T. L. Roach and J. T. Bernhard, "Investigation of sidelobe level performance in phased arrays with pattern reconfigurable elements," *IEEE Antennas Propag. Soc. Int. Symp. Digest*, pp. 105-108, Jun. 2007.
- [22] J. C. Wu, C. C. Chang, T. Y. Chin, S. Y. Huang and S. F. Chang, "Sidelobe level reduction in wide-angle scanning array system using pattern-reconfigurable antennas," *IEEE Int. Microw. Symp. Digest.*, pp.1274-1277, May 2010.
- [23] M. P. Daly and J. T. Bernhard, "Beam steering in pattern reconfigurable arrays using directional modulation," *IEEE Trans. Antennas and Propag.*, vol.58, no.7, pp.2259-2265, Jul. 2010.
- [24] Y. Y. Bai, S. Xiao, M. C. Tang, Z. F. Ding and B. Z. Wang, "Wide-angle scanning phased array with pattern reconfigurable elements," *IEEE Trans. Antennas and Propag.*, vol.59, no.11, pp.4071-4076, Nov. 2011.
- [25] J. Zhang; X. S. Yang, J. L. Li and B. Z. Wang, "A linear phased array with reconfigurable dynamic Yagi-Uda patch antenna elements," *Proc. 2012 Int. Workshop on Microwave and Millimeter Wave Circuits and System Technology (MMWCST)*, pp.1,4, 19-20 Apr. 2012.

- [26] Z. Li, D. Rodrigo, L. Jofre and B. A. Cetiner, "A new class of antenna array with a reconfigurable element factor," *IEEE Trans. Antennas and Propag.*, vol. 61, no. 4, pp.1947-1955, Apr. 2013.
- [27] N. Ramli, M. T. Ali, M. T. Islam, A. L. Yusof and S. Muhamud-Kayat, "Aperture-coupled frequency and patterns reconfigurable microstrip stacked array antenna," *IEEE Trans. Antennas and Propag.*, vol. 63, no. 3, pp.1067-1074, Mar. 2015.
- [28] S. Xiao, C. Zheng, M. Li, J. Xiong and B. Z. Wang, "Varactor-loaded pattern reconfigurable array for wide-angle scanning with low gain fluctuation," *IEEE Trans. Antennas and Propag.*, vol. 63, no. 5, pp.2364-2369, May. 2015.
- [29] CST GmbH, Darmstadt, Germany [Online]. Available: <http://www.cst.com>.
- [30] Satimo, StarLab, Courtaboeuf, France [Online]. Available: <http://www.satimo.com>.
- [31] P. Deo, A. Mehta, D. Mirshekar-Syahkal, P. J. Messy and H. Nakano, "Thickness reduction and performance enhancement of steerable square loop antenna using hybrid high impedance surface," *IEEE Trans. Antennas and Propag.*, vol. 58, no. 5, pp. 1477-1485, May, 2010.
- [32] M.E. Marhic, A. Mehta and A. Pal, "Theory and generation of circularly polarized waves by antenna arrays with N-fold rotational symmetry", *IEEE Antennas Wireless Propag. Lett.*, vol.10, pp. 1441-1444, Nov. 2011.
- [33] A. Pal, A. Mehta and M. E. Marhic, "Generating a pure circularly polarised axial beam from a pattern reconfigurable square loop antenna," *IET Proc.-Microwaves, Antennas & Propagation*, vol.7, no.3, pp.208-213, Feb. 2013.
- [34] C. A. Balanis, "Antenna theory: analysis and design, 3rd edition", Wiley-Inter-science, Hoboken, New Jersey, 2005.
- [35] A. Raaza, A. Mehta, D. Mirshekar-Syahkal and P. J. Massey, "A novel 8 feed beam switched antenna," *Int. Symp. Antennas and Propag. Soc. Digest*, pp.1-4, 5-11 July 2008.



Arpan Pal (M'09) received the Ph.D. degree in advanced telecommunications from Swansea University, Swansea, U.K., in 2013. He worked as a Research Assistant at the Indian Institute of Science (IISc), Bangalore, India, from 2005 to 2006 and at Swansea University, in 2008. Thereafter, he worked as a Lecturer at the Asansol Engineering College, West Bengal, India. In 2014, He was a Research Assistant at The Institute of Electronics Communications and Information Technology (ECIT), Queen's University of Belfast, Belfast, U.K. Since December 2014, he has been a Research Assistant at Antenna and Smart City Lab, Swansea University, U.K. His research interest involves beam-steerable antennas, phased array antennas, frequency selective surface and surface-integrated waveguide antennas.



Amit Mehta (M'05 - SM'11) received the B.Eng. degree in electronics and telecommunication from the University of Pune, India, in 1998 and the M.Sc. degree in telecommunications and information networks and the Ph.D. degree in smart reconfigurable antennas from the University of Essex, U.K., in 2002 and 2005, respectively. From 1998 to 2001, he worked in the Telecommunications Industry in Bangalore and Singapore. From July 2002 to February 2006, he was a Senior Research Officer at the University of Essex. Since February 2006, he has been working at Swansea University, Swansea, U.K. and is the

director of the RF research group where his core research focus is wireless communications, microwave systems and antennas. He is particularly interested in GNSS, body-wearable adaptable antennas, satellite communications, smart antennas, 4G, and millimeter waves. He has successfully supervised over 20 postgraduate research theses and has over 80 technical publications and three patents on invention of the steerable beam smart antenna and concealed weapons detection system.



Dariush Mirshekar-Syahkal received the B.Sc. degree (with distinction) in electrical engineering from Tehran University, Tehran, Iran, in 1974 and the M.Sc. degree in microwaves and modern optics and the Ph.D. degree from University College London, University of London, U.K., in 1975 and 1979, respectively. From 1979 to 1984, he worked as a Research Fellow at University College London, on analysis and design of microwave and millimeter-wave planar transmission lines and components as well as on nondestructive evaluation of materials by electromagnetic techniques. Since 1984, he has been on the staff at the University of Essex, Colchester, UK, where he is a Professor and the Head of RF & Microwave Research Laboratory in the School of Computer Science and Electronic Engineering. He owns several patents and has numerous technical publications including a book entitled *Spectral Domain Method for Microwave Integrated Circuits* (New York: Wiley, 1990). He has been consultant to more than 10 major international companies. His current research encompasses adaptive antennas, super-compact RF filters, RF amplifier linearizations, characterization and applications of liquid crystal materials at microwave and mm-wave frequencies, and numerical modelling in electromagnetics and circuits. Professor Mirshekar is a Fellow of the IEEE, a Fellow of the IET, and a Chartered Engineer.



Hisamatsu Nakano (M'75-SM'87-F'92-LF'11) received the Dr. E. degree from Hosei University, Tokyo, Japan, in 1974. Since 1973, he has been a member of the faculty of Hosei University, where he is now a professor emeritus and a special appointment researcher at the graduate school topical research center of the same university. His research topics include numerical methods for low- and high-frequency antennas and optical waveguides. Prof. Nakano received the IEEE TRANSACTIONS ON ANTENNAS AND PROPAGATION H. A. Wheeler Award in 1994. He was also the recipient of the IEEE Antennas and Propagation Society Chen-To Tai Distinguished Educator Award in 2006 and the recipient of the Prize for Science and Technology (from Japan's Minister of Education, Culture, Sports, Science, and Technology) in 2010. In 2016, he received the IEEE Antennas Propagation Society Distinguished Achievement Award. He is an Associate Editor of several journals and magazines, such as *Electromagnetics* and the *IEEE Antennas and Propagation Magazine*. Prof. Nakano served as a member of the IEEE APS administrative committee (2000-2002) and a Region 10 Representative(2001-2010).